Hindawi
Complexity
Volume 2019, Article ID 5920187, 15 pages
https://doi.org/10.1155/2019/5920187

Research Article

Information Spreading on Weighted Multiplex Social Network

Xuzhen Zhu,[1] **Jinming Ma**,[1] **Xin Su**,[2] **Hui Tian**,[1] **Wei Wang**,[3] **and Shimin Cai**[4]

[1]*State Key Laboratory of Networking and Switching Technology, Beijing University of Posts and Telecommunications, Beijing 100876, China*
[2]*School of Economics and Management, Beijing University of Posts and Telecommunications, Beijing 100876, China*
[3]*Cybersecurity Research Institute, Sichuan University, Chengdu 610065, China*
[4]*Web Sciences Center, School of Computer Science and Engineering, University of Electronic Science and Technology of China, Chengdu 611731, China*

Correspondence should be addressed to Wei Wang; wwzqbx@hotmail.com

Received 29 July 2019; Revised 15 October 2019; Accepted 28 October 2019; Published 11 November 2019

Academic Editor: Eric Campos-Canton

Information spreading on multiplex networks has been investigated widely. For multiplex networks, the relations of each layer possess different extents of intimacy, which can be described as weighted multiplex networks. Nevertheless, the effect of weighted multiplex network structures on information spreading has not been analyzed comprehensively. We herein propose an information spreading model on a weighted multiplex network. Then, we develop an edge-weight-based compartmental theory to describe the spreading dynamics. We discover that under any adoption threshold of two subnetworks, reducing weight distribution heterogeneity does not alter the growth pattern of the final adoption size versus information transmission probability while accelerating information spreading. For fixed weight distribution, the growth pattern changes with the heterogeneous of degree distribution. There is a critical initial seed size, below which no global information outbreak can occur. Extensive numerical simulations affirm that the theoretical predictions agree well with the numerical results.

1. Introduction

The Internet [1, 2], web 2.0 [3], and intelligent mobile terminals [4] have completely transformed people's daily lives; these infrastructures have assisted people in constructing virtual social networks [5–8], which map people's connections in real life into virtual cyberspaces and extend people's social scope significantly, not only with schoolmates, colleagues, and family members, but also with strangers in different countries. Previously, various types of social networks such as Facebook [9], Twitter [10], Weibo [11], and Wechat [12] have been used. Social networks are important in information transmission between users [13], such as commodity recommendation [14], news spreading [15, 16], advertisement diffusion [17, 18], health behavior adoption [19], discovery of new friends [20], and social innovation propagation [21]. In addition, understanding the mechanism of information spreading in social networks can facilitate in the design of antivirus strategies [22–24], control rumors [25], avoid economic risks [26, 27], restrain social unrest [28], etc. Because of important values in economic activities and engineering applications, social information spreading has attracted significant attention [28–32].

Based on complex network theory [33, 34], regarding a user as a node and a connective relation as an edge [35], researchers have mined various underlying factors to investigate the information spreading mechanism and unveil the fundamental laws. Wide-ranging factors have been investigated, such as the initial seed size [36], clustering coefficient [37], community structure [38], temporal network [39], role of synergy [40, 41], heterogeneous adoption thresholds [42], and limited imitation [43–45]. Additionally, information spreading on a multiplex network [46–48] has aroused the interest of researchers who perform numerous investigations about communication channel alternations on multiplex networks [49], heterogeneous behavioral adoption on multiplex networks [16], opinion competition on multiplex networks [50], effect of multiple social

networks on user awareness [51], social support for suppressing epidemics on multiplex networks [52], the interplay of social influence in multiplex networks [53], replicator dynamics on multiplex networks [54], etc.

Moreover, in social networks, because of multiple confirmations of the credibility and legitimacy of information, information spreading exhibits the effect of social reinforcement [55, 56]. Repeated transmission of the same information from one neighbor cannot enhance the credibility nor facilitate adoption. Therefore, social reinforcement derived from the memory of nonredundant information has been investigated [57], which should be considered in information spreading. Apart from the abovementioned factors, edges represent the connective relations between users and are always modeled in a binary state [58]. In real social networks, different types of individuals, such as colleagues, schoolmates, family members, and strangers may have intimate or distant relations. Even for the same type of individuals, they may exhibit different extents of intimacy. Therefore, similar to epidemic spreading on a weighted network [59], the relations in a social network should be reasonably modeled as weighted edges [60, 61]. Noticeably, compared with a one-layered complex network, research on information spreading in multiplex networks is more complicated and challenging. Apart from the intraheterogeneity of weights between edges in the same layer, interheterogeneity of weight distributions between two layers exists as well. Unfortunately, studies performed hitherto lack profound analysis regarding information spreading on weighted multiplex networks with social reinforcement derived from the memory of nonredundant information.

Herein, in terms of social reinforcement effect generated from the memory of nonredundant information and heterogeneous weight distributions in two subnetworks, we propose an information spreading model on a weighted multiplex network. To further understand the intrinsic mechanism of information spreading and quantitatively predict the effects of spreading in time evolution and final steady state, we develop an edge-weight-based compartmental theory. Extensive simulations based on our proposed numerical method suggest that theoretical predictions agree well with numerical simulations. Combining the theoretical predictions and numerical simulations, we discovered that reducing weight distribution heterogeneity does not alter the growth pattern of the final adoption size but can accelerate information spreading and promote the outbreak of information spreading. Furthermore, we discovered that a critical seed size determines the global information outbreak, above which reducing the weight distribution heterogeneity materially affects the facilitation of information spreading. Additionally, reducing the degree distribution heterogeneity can alter the growth pattern of the final adoption size $R(\infty)$.

The remainder of the paper is organized as follows: In Section 2, we describe the information spreading model on a weighted multiplex network. In Section 3, we propose an edge-weight-based compartmental theory to analyze information spreading on a weighted multiplex network. In Section 4, the numerical simulation method and parameter settings are introduced. In Section 5, we compare the theoretical predictions with the numerical simulation results and unveil the effect mechanism of the weighted multiplex network structure on information spreading. In Section 6, conclusions are presented.

2. Model Descriptions

For investigating information spreading on a weighted multiplex social network, we constructed an information spreading model based on an N-node two-layer weighted multiplex network, in which layers A and B represent two different independent social networks (illustrated in Figure 1). Correlated nodes in two layers indicate that they are the same individual, and edges between nodes in each subnetwork represent interindividual social relations. To eliminate the unnecessary intradegree-degree correlation, the uncorrelated configuration model [62] was manipulated to construct the multiplex network following two independent degree distributions $P_A(k_i^A)$ and $P_B(k_i^B)$, in which k_i^A and k_i^B indicate the degrees of node i in layer A and B, respectively. The degree vector of node i is set as $\overrightarrow{k_i} = (k_i^A, k_i^B)$. In this paper, we assume that there is no correlation between the degree and weight distributions and the joint degree distribution is $P(\overrightarrow{k_i}) = P_A(k_i^A)P_B(k_i^B)$. Self-loop and multiple edges are forbidden. Regarding social reinforcement, we assume that each individual has different adoption willingness in different social subnetworks. Consequently, node i, representing an arbitrary individual, has adoption thresholds T_A and T_B in layers A and B, respectively, and a smaller adoption threshold suggests more considerable information adoption willingness. Moreover, the intimate relations between individuals typically hold different strengths in the same social subnetwork and in two distinctive subnetworks. Therefore, we further construct the weighted multiplex network with two dependent edge-weight distributions, $g_A(w)$ and $g_B(w)$. Subsequently, if an edge with weight w_{ij}^X exists between nodes i and j in the layer $X \in \{A, B\}$, individual i in the subnetwork X transmits the information to j with probability

$$\lambda_X\left(w_{ij}^X\right) = 1 - \left(1 - \beta_X\right)^{w_{ij}^X}, \tag{1}$$

where β_X is the unit transmission probability in the subnetwork $X \in \{A, B\}$. Given β_X, enlarging w_{ij}^X can monotonically increase $\lambda_X(w_{ij}^X)$, which coincides with the positive correlation between relationship weight and transmission preference.

In real social networks, individuals always trustfully adopt information after receiving a certain number of it from distinctive neighbors, owing to social reinforcement originating from the memory of nonredundant information transmission [57]. Accordingly, we applied the generalized susceptible-adopted-recovered (SAR) model to describe the state of an individual at each time step in the information spreading process. At the same time step, an individual can only remain in one state: S-state (susceptible), A-state (adopted), or R-state (recovered). The S-state implies that an

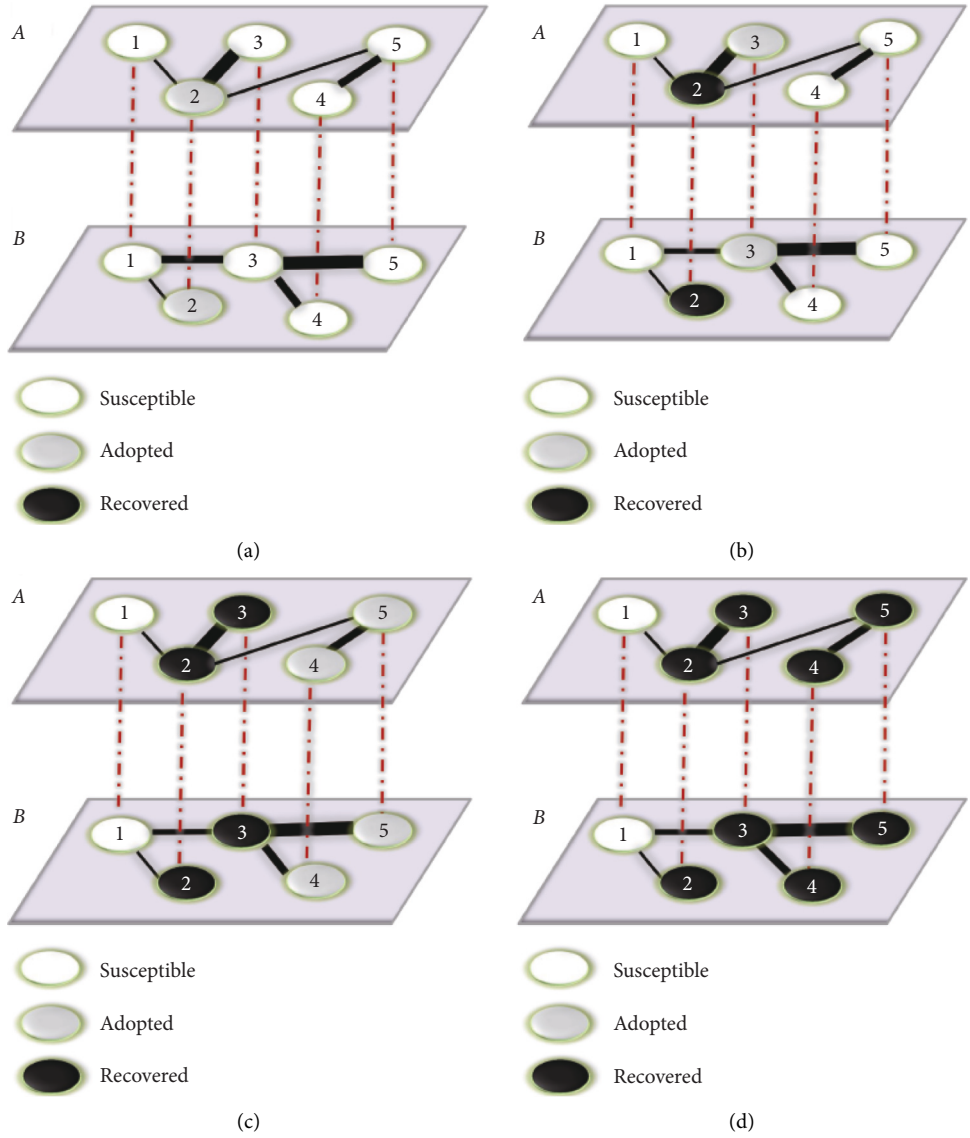

Figure 1: Illustration of social information spreading with transformation of three states (susceptible, adopted, and recovered) on a weighted multiplex network. Two different independent social networks A and B, comprising degrees of intimate relations, represent two layers of the weighted multiplex network, in which different degrees of edge-widths denote different edge-weights.

individual has not adopted the information. The A-state indicates that an individual has adopted the information and can transmit the information to neighbors. The R-state means that an individual has lost interest in the information and stops diffusion.

Furthermore, the detailed information spreading process is as follows: Initially, randomly selecting a fraction ρ_0 of nodes as initial seeds (in the A-state). At each time step, each A-state node i attempts to transmit the information to its S-state neighbor j simultaneously through an edge of weight w_{ij}^A with probability $\lambda_A(w_{ij}^A)$ in layer A and through an edge of weight w_{ij}^B with probability $\lambda_B(w_{ij}^B)$ in layer B according to equation (1). Because of nonredundant information transmission, once an edge between nodes i and j in layer A or B successfully delivers the information from i to j, such an edge is not allowed for repeated information delivery. An adopted node, however, can perform many attempts until it turns into the R-state. If the S-state node j in the layer $X \in \{A, B\}$ successfully receives one piece of information from the A-state neighbor node j, its accumulative number m_j^X of information pieces in the layer $X \in \{A, B\}$ will increase by one, i.e., $m_j^X \longrightarrow m_j^X + 1$. Then, node j will compare the accumulative number m_j^X with its adoption threshold T_X. In reality, for confirming the legitimacy and credibility of the information, an individual can adopt the information only if he/she corroborates with the information in both subnetworks. Therefore, the susceptible node j can enter the A-state when $m_j^A \geq T_A$ and $m_j^B \geq T_B$ co-occur in both layers A and B; otherwise, it remains in the S-state. Regarding social reinforcement, because the accumulative number of information pieces determines the information adoption, the information spreading process is characterized by the

non-Markovian effect. At the same time step, after information transmission, the A-state node j will lose interest in the information and enter the R-state with probability γ, i.e., it will stop diffusing information in both layers A and B. Once the node changes into the R-state, it will retreat from further information spreading. Finally, the disappearance of all A-state nodes signals the termination of the spreading dynamics.

3. Edge-Weight-Based Compartmental Theory

To include the social reinforcement effect, the mean-filed theory [63] and an advanced approach [64] can be used. Inspired by References [57, 65, 66], an edge-weight-based compartmental theory is conceived to analyze the spreading process with theoretically strong correlation among the three states of nodes in a multiplex the network featured by strong weight heterogeneity. The theory assumes that the information spreading is on large, sparse, uncorrelated, and local tree-like weighted multiplex networks.

In the edge-weight-based compartmental theory, a node in the cavity state [67] implies that it can only receive information from but cannot transmit information to its neighbors. We denote $\theta_X(t)(X \in \{A, B\})$ as the probability that the information has not been passed to the S-state neighbors alongside a randomly selected edge in layer X by time t. Furthermore, in a weight multiplex network, we denote $\theta_w^X(t)$ as the probability that a node has not been informed through a randomly selected edge with weight w in layer X by time t. Following weight distribution $g_A(w)$ in layer A and $g_B(w)$ in layer B, we can obtain

$$\theta_A(t) = \sum_w g_A(w)\theta_w^A(t), \tag{2}$$

$$\theta_B(t) = \sum_w g_B(w)\theta_w^B(t). \tag{3}$$

An arbitrary S-state node i with degree vector $\overrightarrow{k_i} = (k_i^A, k_i^B)$ receives m_A and m_B pieces of information by time t with the probabilities

$$\begin{aligned}\phi_{m_A}^A\left(k_i^A, t\right) &= \binom{k_i^A}{m_A}\theta_A(t)^{k_i^A - m_A}\left[1 - \theta_A(t)\right]^{m_A}\\ \phi_{m_B}^B\left(k_i^B, t\right) &= \binom{k_i^B}{m_B}\theta_B(t)^{k_i^B - m_B}\left[1 - \theta_B(t)\right]^{m_B}\end{aligned} \tag{4}$$

respectively.

As mentioned in Section 2, an S-state node with degree vector $\overrightarrow{k} = (k^A, k^B)$ can adopt the information only if the cumulative numbers $m_A \geq T_A$ and $m_B \geq T_B$ occur simultaneously; inversely, the S-state node having received m_A and m_B pieces of information by time t will remain in the S-state with probability

$$\begin{aligned}s(\overrightarrow{k}, t) = (1 - \rho_0)\Bigg[1 - \Bigg(1 - \sum_{m_A=0}^{T_A-1}\phi_{m_A}^A\left(k^A, t\right)\Bigg)\\ \times\Bigg(1 - \sum_{m_B=0}^{T_B-1}\phi_{m_B}^B\left(k^B, t\right)\Bigg)\Bigg].\end{aligned} \tag{5}$$

We define the probability that a susceptible node with any degree in the layer $X \in \{A, B\}$ remaining in the S-state if it receives m_X pieces of information by time t as

$$\eta_X(t) = \sum_{k^X} P_X\left(k^X\right)\sum_{m_X=0}^{T_X-1}\phi_{m_X}^X\left(k^X, t\right). \tag{6}$$

Furthermore, the fraction of nodes in the S-state at time t can be expressed as

$$\begin{aligned}S(t) &= \sum_{\overrightarrow{k}} P(\overrightarrow{k})s(\overrightarrow{k}, t)\\ &= (1 - \rho_0)(\eta_A + \eta_B - \eta_A\eta_B).\end{aligned} \tag{7}$$

If we wish to obtain $S(t)$, we should solve $\theta_X(t)$, which depends on $\theta_w^X(t)$ in a weighted network. Therefore, we focus on $\theta_w^X(t)$ at first. According to [57], in layer X, the neighbor connected by an edge with weight w to a node in the cavity state can be in the S-state, A-state, or R-state; therefore, $\theta_w^X(t)(X \in \{A, B\})$ comprises the following three parts:

$$\theta_w^X(t) = \xi_{S,w}^X(t) + \xi_{A,w}^X(t) + \xi_{R,w}^X(t), \tag{8}$$

where $\xi_{S,w}^X(t)$, $\xi_{A,w}^X(t)$, and $\xi_{R,w}^X(t)$ indicate the probabilities that a neighbor connected by an edge with weight w to a node in the cavity state remains in the S-, A-, and R-states, respectively, and has not transmitted information by time t.

If neighbor j with degree vector $\overrightarrow{k_j} = (k_j^A, k_j^B)$ is linked by an edge of weight w to the node i in the cavity state in layer $A(B)$, then neighbor j can only receive information from other $k_j^A - 1(k_j^B - 1)$ edges in layer $A(B)$. Therefore, neighbor j receives n_A pieces of information in layer A with probability $\phi_{n_A}(k_j^A - 1, t)$ and, with no constraint in layer B, receives n_B pieces of information in layer B with probability $\phi_{n_V}(k_j^B, t)$. Subsequently, neighbor j remains in the S-state in layer A with probability

$$\begin{aligned}\Theta_A\left(\overrightarrow{k_j}, t\right) = 1 - \Bigg[1 - \sum_{n_A=0}^{T_A-1}\phi_{n_A}\left(k_j^A - 1, t\right)\Bigg]\\ \times\Bigg[1 - \sum_{n_B=0}^{T_B-1}\phi_{n_B}\left(k_j^B, t\right)\Bigg].\end{aligned} \tag{9}$$

Analogously, neighbor j is connected with node i by an edge with weight w in layer B and remains in the S-state with probability

$$\begin{aligned}\Theta_B\left(\overrightarrow{k_j}, t\right) = 1 - \Bigg[1 - \sum_{n_A=0}^{T_A-1}\phi_{n_A}\left(k_j^A, t\right)\Bigg]\\ \times\Bigg[1 - \sum_{n_B=0}^{T_B-1}\phi_{n_B}\left(k_j^B - 1, t\right)\Bigg].\end{aligned} \tag{10}$$

Accordingly, given the joint degree distribution $p(\overrightarrow{k})$, in layer X, an edge with weight w connects to an S-state neighbor j with probability

$$\xi^X_{S,w}(t) = (1-\rho_0)\frac{\sum_{\overrightarrow{k_j}} k_j^X p\left(\overrightarrow{k_j}\right)\Theta_X\left(\overrightarrow{k_j}, t\right)}{\langle k_j^X\rangle}, \tag{11}$$

where the expression $k_j^X p(\overrightarrow{k_j})/\langle k_j^X\rangle$ denotes the probability an edge connecting to a neighbor with degree k_j^X in layer X.

Next, we proceed with the evolution of $\xi^X_{A,w}(t)$ and $\xi^X_{R,w}(t)$ in the layer $X \in \{A, B\}$. If, through an edge with weight w, the information is successfully transmitted to the neighbor in layer X with probability λ_w^X, the change in $\theta_w^X(t)$ is calculated as

$$\frac{\mathrm{d}\theta_w^X(t)}{\mathrm{d}t} = -\lambda_w^X \xi^X_{A,w}(t). \tag{12}$$

If neighbor j in the A-state has not transmitted information to node i through an edge of weight w with probability $(1-\lambda_w^X)$ in layer X but enters into the R-state with probability γ at time t, the value of $\xi^X_{R,w}(t)$ will increase, and thus the dynamical differential value of $\xi^X_{R,w}(t)$ can be obtained by

$$\frac{\mathrm{d}\xi^X_{R,w}(t)}{\mathrm{d}t} = \gamma\left(1-\lambda_w^X\right)\xi^X_{A,w}(t). \tag{13}$$

The initial conditions are $\theta_w^X(0) = 1$ and $\xi^X_{R,w}(0) = 0$; therefore, combining equation (12) with (13), we can obtain

$$\xi^X_{R,w}(t) = \frac{\gamma\left(1-\lambda_w^X\right)\left[1-\theta_w^X(t)\right]}{\lambda_w^X}. \tag{14}$$

After inserting equations (11) and (14) into equation (8), we can obtain

$$\xi^X_{A,w}(t) = \theta_w^X(t) - (1-\rho_0)\frac{\sum_{\overrightarrow{k_j}} k_j^X P\left(\overrightarrow{k_j}\right)\Theta_X\left(\overrightarrow{k_j}, t\right)}{\langle k_j^X\rangle} - \frac{\gamma\left(1-\lambda_w^X\right)\left[1-\theta_w^X(t)\right]}{\lambda_w^X}. \tag{15}$$

In equation (15), substituting $\xi^X_{A,w}(t)$ with $(1/-\lambda_w^X)(\mathrm{d}\theta_w^X(t)/\mathrm{d}t)$ according to equation (8), we further deduce

$$\frac{\mathrm{d}\theta_w^X(t)}{\mathrm{d}t} = \lambda_w^X(1-\rho_0)\frac{\sum_{\overrightarrow{k_j}} k_j^X P\left(\overrightarrow{k_j}\right)\Theta_X\left(k_j^X, t\right)}{\langle k_j^X\rangle} + \gamma\left(1-\lambda_w^X\right) - \left[\gamma + (1-\gamma)\lambda_w^X\right]\theta_w^X(t). \tag{16}$$

When $t \longrightarrow \infty$, $\mathrm{d}\theta_w^X(t)/\mathrm{d}t = 0$, and we have the steady-state value $\theta_w^X(\infty)$ as

$$\theta_w^X(\infty) = \frac{\lambda_w^X(1-\rho_0)\sum_{\overrightarrow{k_j}} k_j^X P\left(\overrightarrow{k_j}\right)\Theta_X\left(\overrightarrow{k_j}, \infty\right) + \langle k_j^X\rangle\gamma\left(1-\lambda_w^X\right)}{\langle k_j^X\rangle\left[\gamma + (1-\gamma)\lambda_w^X\right]}. \tag{17}$$

Inserting $\theta_w^X(\infty)$ into equations (2) and (3), we thus obtain

$$\theta_X(\infty) = \sum_w g_X(w)\theta_w^X(\infty) = f_X\left(\theta_A(\infty), \theta_B(\infty)\right). \tag{18}$$

For a convenient expression, we rewrite $\theta_A(\infty) = f_A(\theta_A(\infty), \theta_A(\infty))$ as

$$\theta_A = F_A(\theta_B), \tag{19}$$

and $\theta_B(\infty) = f_B(\theta_A(\infty), \theta_B(\infty))$ as

$$\theta_B = F_B(\theta_A). \tag{20}$$

A discontinuous growth pattern will occur [68] when equation (19) is tangent to equation (20) with $\theta_A < 1$ and $\theta_B < 1$. Moreover, critical conditions can be acquired from the following equation:

$$\frac{\partial f_A\left(\theta_A(\infty), \theta_B(\infty)\right)}{\partial\theta_B(\infty)}\frac{\partial f_B\left(\theta_A(\infty), \theta_B(\infty)\right)}{\partial\theta_A(\infty)} = 1. \tag{21}$$

From the theoretical analysis above, the general solutions for adoption thresholds T_A and T_B can be derived, but the theoretical analysis itself may not be easily comprehended. Therefore, an intuitive illustration exemplifies the general theory with a particular case, i.e., $T_A = T_B = 1$. In this case, equations (9) and (10) are rewritten as

$$\Theta_A\left(\overrightarrow{k_j}, t\right) = \theta_A(t)^{k_j^A - 1} + \theta_B(t)^{k_j^B} - \theta_A(t)^{k_j^A - 1}\theta_B(t)^{k_j^B},$$
$$\Theta_B\left(\overrightarrow{k_j}, t\right) = \theta_A(t)^{k_j^A} + \theta_B(t)^{k_j^B - 1} - \theta_A(t)^{k_j^A}\theta_B(t)^{k_j^B - 1}. \tag{22}$$

Owing to independence, we obtain $P(\overrightarrow{k_j}) = P(k_j^A)P(k_j^B)$ and substitute (23) and (24) into equation (17) as follows:

$$\theta_w^A(\infty) = \frac{\lambda_w^A(1-\rho_0)\left[H_A^1(\theta_A(\infty)) + H_B^0(\theta_B(\infty)) - H_{AB}^{1,0}(\theta_A(\infty), \theta_B(\infty))\right]}{\left[\gamma + (1-\gamma)\lambda_w^A\right]} + \frac{\gamma\left(1-\lambda_w^A\right)}{\left[\gamma + (1-\gamma)\lambda_w^A\right]}, \tag{23}$$

$$\theta_w^B(\infty) = \frac{\lambda_w^B(1-\rho_0)\left[H_A^0(\theta_B(\infty)) + H_B^1(\theta_A(\infty)) - H_{AB}^{0,1}(\theta_A(\infty), \theta_B(\infty))\right]}{\left[\gamma + (1-\gamma)\lambda_w^B\right]} + \frac{\gamma\left(1-\lambda_w^B\right)}{\left[\gamma + (1-\gamma)\lambda_w^B\right]}, \tag{24}$$

where $H_X^0(x) = \sum_{k_X} P_X(k_X) x^{k_X}$ represents the generation function of degree distribution $P_X(k_X), X \in \{A, B\}$, and $H_X^1(x) = ((\sum_{k_X} k_X P(k_X) x^{k_X - 1})/\langle k_X \rangle), X \in \{A, B\}$ represents the generation function of excess degree distribution $P_X(k_X)$. Additionally, the generation functions of degree distribution $P(\overrightarrow{k})$ are expressed as follows:

$$H_{AB}^{1,0}(x, y) = \frac{1}{H'_{A0}(1)} \frac{\partial H_{AB}^{0,0}(x, y)}{\partial x},$$

$$H_{AB}^{0,1}(x, y) = \frac{1}{H'_{B0}(1)} \frac{\partial H_{AB}^{0,0}(x, y)}{\partial y}, \tag{25}$$

$$H_{AB}^{0,0}(x, y) = \sum_{k_A, k_B} P(\overrightarrow{k}) x^{k_A} y^{k_B},$$

where $\overrightarrow{k} = (k_A, k_B)$. Subsequently, substituting equations (23) and (24) into equation (21), we can deduce the critical conditions.

4. Numerical Method

Based on Erdös–Rényi (ER) [69] and the scale-free (SF) [62] random network model, extensive numerical simulations on artificial two-layer networks were performed to verify the theoretical analysis above. Without loss of generality, we set the network size $N = 10^4$ and mean-degree $\langle k \rangle_A = \langle k \rangle_B = \langle k \rangle = 10$. For convenience, the information transmission unit probability in the two layers is set as $\beta_A = \beta_B = \beta$. Additionally, the weight distribution of the network layer $X \in \{A, B\}$ follows $g_X(\omega) \sim \omega^{-\alpha_\omega^X}$ with $\omega_X^{\max} \sim N^{1/(\alpha_\omega^X - 1)}$ and mean weight $\langle \omega \rangle_A = \langle \omega \rangle_B = \langle \omega \rangle = 8$. At the steady state in which no node in the A-state exists, we compute the spreading range by measuring the fraction of nodes in the R-state $R(\infty)$. The simulation results are obtained by averaging over at least 10^4 independent dynamical realizations on 30 artificial networks.

To obtain the critical condition from the simulations, the *relative variance* χ [70] is applied in our numerical verification, using the following method:

$$\chi = N \frac{\langle R(\infty)^2 \rangle - \langle R(\infty) \rangle^2}{\langle R(\infty) \rangle}, \tag{26}$$

where $\langle \ldots \rangle$ is the ensemble average, and $\langle R(\infty) \rangle$ and $\langle R(\infty)^2 \rangle$ are the first and secondary moments of $R(\infty)$, respectively. The peaks of the curve of relative variance χ versus the information transmission probability correspond to the critical points.

5. Results and Discussion

In reality, from the perspective of a degree distribution model, layers in some multiplex social networks exhibit the homogeneous creation mechanism, such as MSN versus ICQ, but layers in other multiplex social networks may exhibit heterogeneous creation mechanisms, such as ICQ versus Facebook. Therefore, from the aspects of homogeneous and heterogeneous degree distributions of two layers, the effects of weight distribution heterogeneity on information spreading in multiplex social networks is discussed in this section in terms of the parameters in Section 4.

5.1. ER-ER Weighted Multiplex Networks. First, we investigate information spreading on a two-layered weighted ER-ER network with Poisson degree distribution $p_A(k_A) = e^{-\langle k_A \rangle} (\langle k_A \rangle^{k_A}/k_A!)$ in layer A and $p_B(k_B) = e^{-\langle k_B \rangle} (\langle k_B \rangle^{k_B}/k_B!)$ in layer B.

We first explore the time evolutions of node densities in three states (S-state, A-state, and R-state) under different weight distribution exponents α_ω^A and α_ω^B, as shown in Figure 2. Under the same information transmission unit probability β but different adoption thresholds and seed sizes, Figure 2 shows the plots of curves with $T_A = 1; T_B = 2; \rho_0 = 0.03$ in the top panel and $T_A = 1; T_B = 3; \rho_0 = 0.1$ in the bottom panel. Regardless of the top or the bottom panel, with time t, the size of $S(t)$ decreases gradually from $1 - \rho_0$ to 0, $A(t)$ changes from ρ_0 to 0 eventually, and $R(t)$ indicating the final adoption size increases gradually from 0 to 1 at the end. With the increase in the weight distribution exponent from $\alpha_\omega^A = 3, \alpha_\omega^B = 2.5$ in Figures 2(a) and 2(e), $\alpha_\omega^A = 3, \alpha_\omega^B = 3$ in Figures 2(b) and 2(f), and $\alpha_\omega^A = 3, \alpha_\omega^B = 3.5$ in Figures 2(c) and 2(g), the evolution time consumed decreases from 19 to 13 in the top panel and 11 to 9 in the bottom panel. Additionally, the final adoption size $R(\infty)$ augments at the same time t (see the comparison in Figures 2(d) and 2(h)). The phenomena occurring during the time evolution suggest that increasing the weight distribution exponent (reducing weight distribution heterogeneity) can facilitate information spreading in a weighted multiplex network.

Next, given the adoption thresholds T_A, T_B, and seed size ρ_0, we investigate the growth pattern of the final adoption size $R(\infty)$ versus information transmission unit probability β. In Figure 3(a), with $T_A = 1$, $T_B = 1$, and $\rho_0 = 0.005$, increasing the weight distribution exponent such as from $\alpha_\omega^A = 3, \alpha_\omega^B = 2.5$ to $\alpha_\omega^A = 3, \alpha_\omega^B = 3.5$ does not change the growth pattern of the final adoption size $R(\infty)$ versus β but reduces the critical information transmission unit probability β_c, which can be numerically captured by the peaks of relative variance χ in Figure 3(e) with the same settings of Figure 3(a). Figure 3(b), with different $T_A = 1; T_B = 2; \rho_0 = 0.03$, exhibits the same pattern as Figure 3(a), with the peaks of relative variance χ in Figure 3(f). Even enlarging the seed size ($\rho_0 = 0.1$) in Figure 3(c) with the same adoption threshold of Figure 3(b), the final adoption size $R(\infty)$ versus β increases in the same pattern regardless of the increase in weight distribution. Besides, keeping the seed size ρ_0 as the same of Figure 3(c) ($\rho_0 = 0.1$), Figure 3(d), with further increase of the adoption threshold $T_A = 1, T_B = 3$, also shows similar phenomena as those in Figures 3(a)–3(c), verified by the peaks of χ in Figure 3(h). The above phenomena suggest that increasing the weight distribution exponent (decreasing weight distribution heterogeneity) will

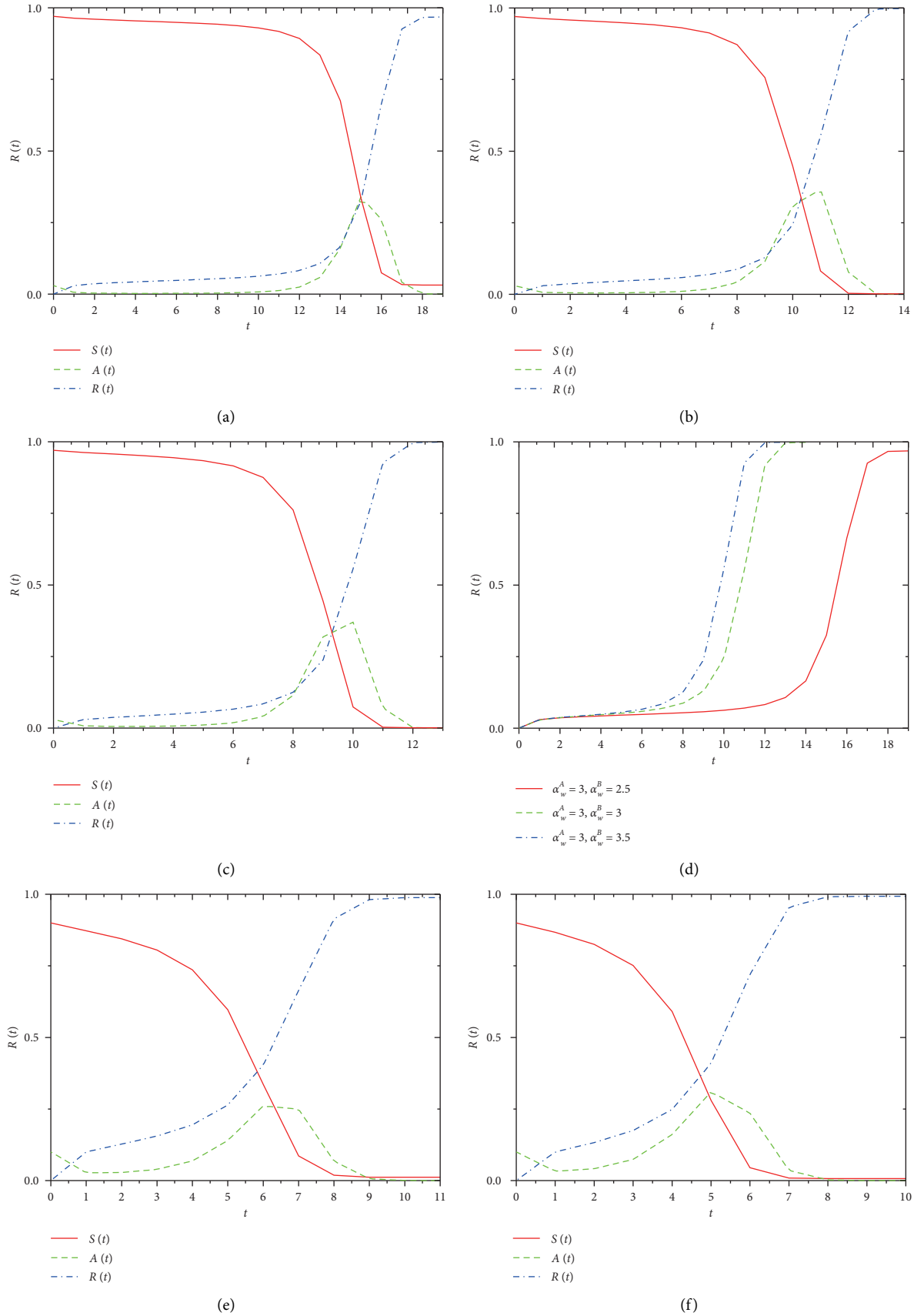

Figure 2: Continued.

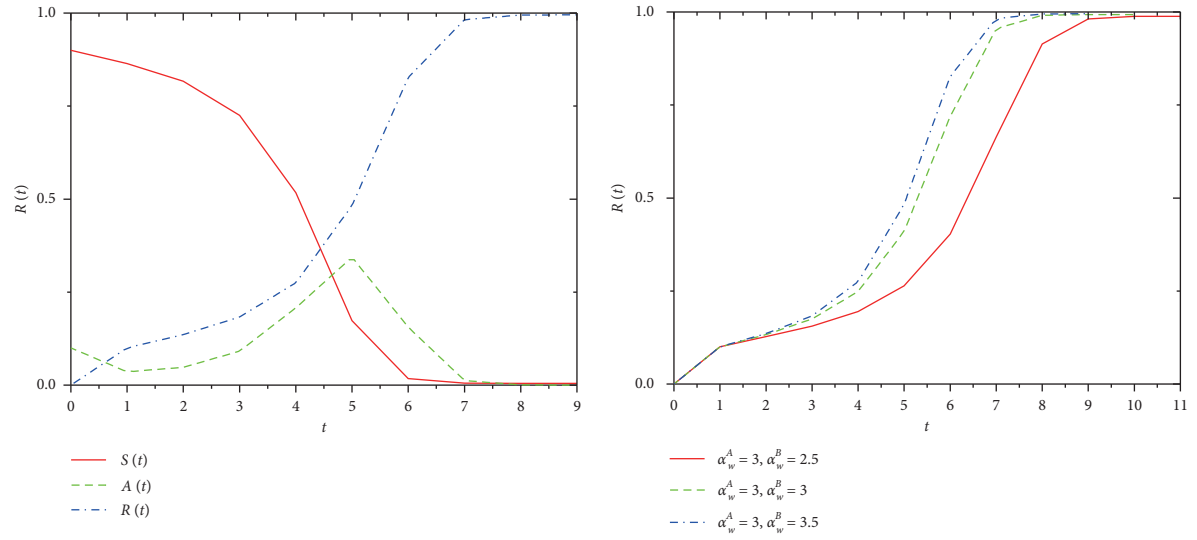

(g) (h)

FIGURE 2: Time evolutions of node densities in three states (S-state, A-state, and R-state) on the ER-ER weighted multiplex network, under different weight distribution exponents α_ω^A and α_ω^B. To unveil the effect of the threshold and seed size, two groups of subgraphs with $T_A = 1; T_B = 2; \rho_0 = 0.03$ and $T_A = 1; T_B = 3; \rho_0 = 0.1$ are shown in the top and bottom panels, respectively. Under the same information transmission unit probability β, subgraphs (a), (b), and (c) from the top panel have similar parameters of $\alpha_\omega^A = 3$, $\alpha_\omega^B = 2.5$; $\alpha_\omega^A = 3$, $\alpha_\omega^B = 3$; and $\alpha_\omega^A = 3$, $\alpha_\omega^B = 3.5$ with (e), (f), and (g), respectively. Particularly, subgraphs (d) and (h) emphasize the time evolution of the R-state node density $R(t)$ under different weight distribution exponents. In both panels, despite the different thresholds and seed sizes, at the same time step, the density of nodes in the R-state under $\alpha_\omega^A = 3, \alpha_\omega^B = 3.5$ exceeds other densities under $\alpha_\omega^A = 3, \alpha_\omega^B = 2.5$ and $\alpha_\omega^A = 3, \alpha_\omega^B = 3$. These phenomena suggest that large weight distribution exponents (small weight distribution heterogeneity) facilitate information spreading. The basic parameters are $N = 10^4$, $\langle k \rangle = 10$, $\langle \omega \rangle = 8$, $\gamma = 1.0$, and $\beta = 0.3$.

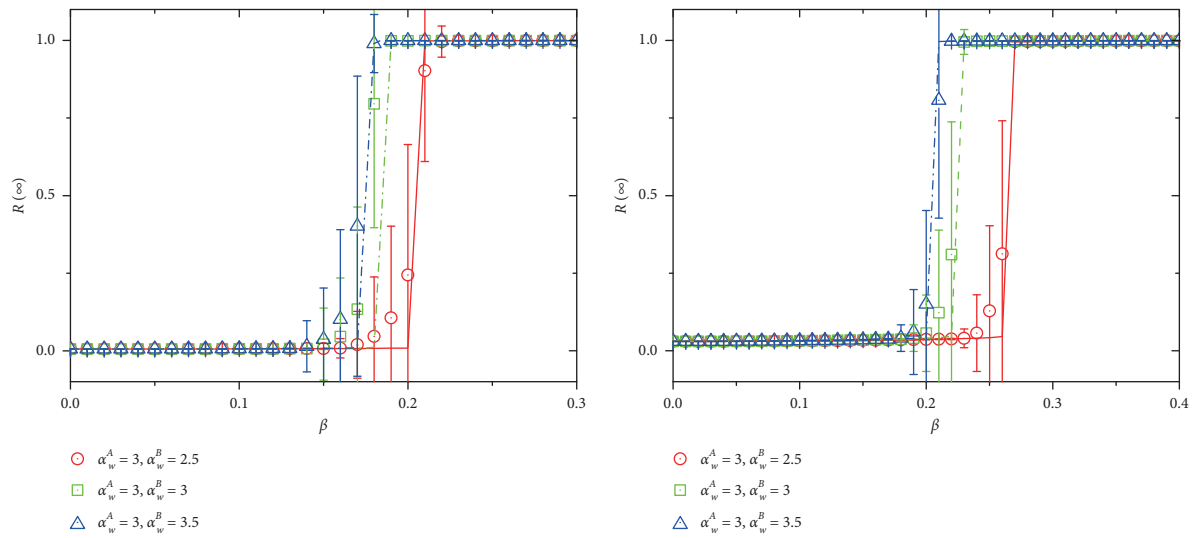

(a) (b)

FIGURE 3: Continued.

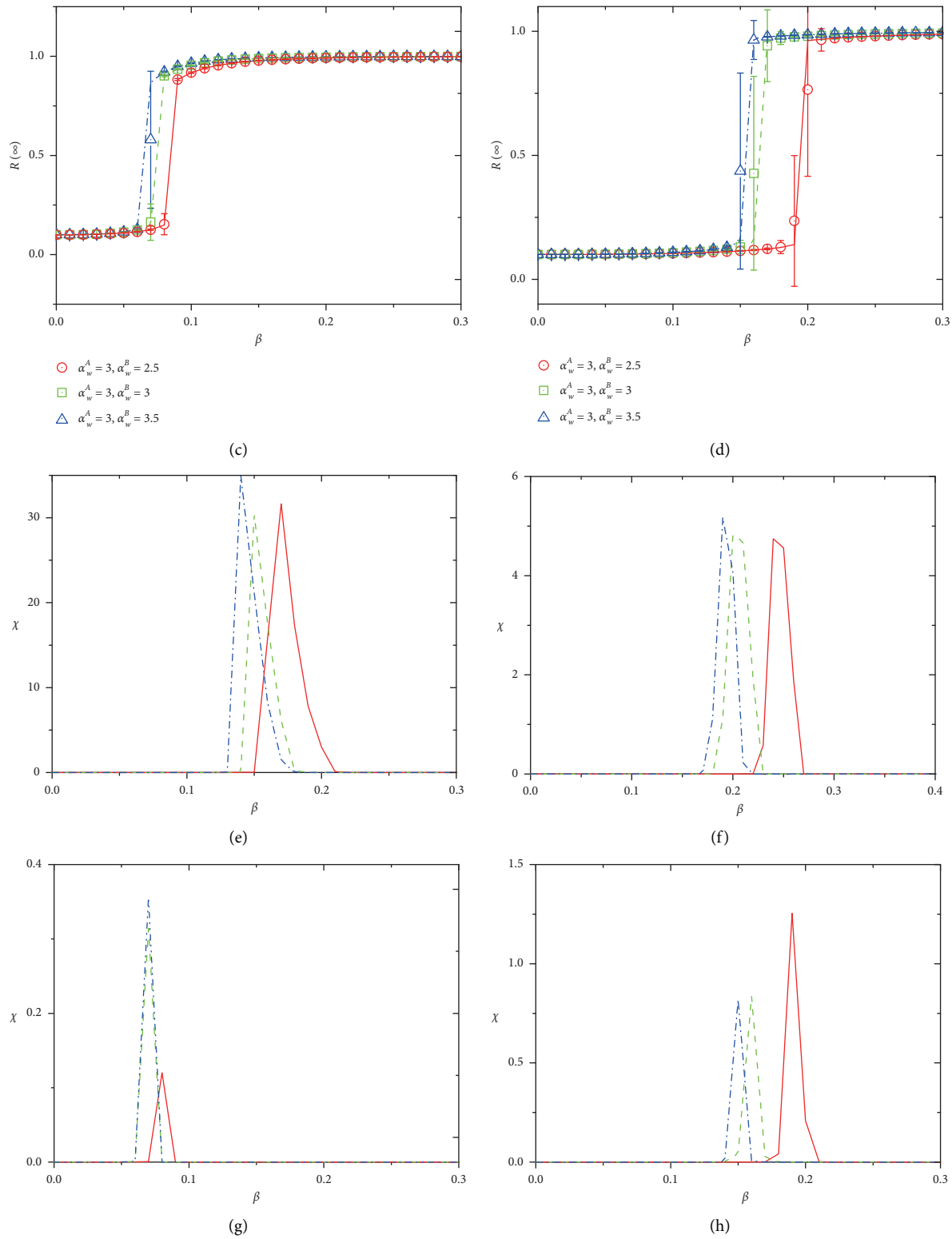

FIGURE 3: Growth pattern of the final adoption size $R(\infty)$ versus information transmission unit probability β on the ER-ER weighted multiplex network, under different weight distribution exponents α_ω^A and α_ω^B, given adoption thresholds (T_A, T_B) and initial fraction ρ_0 of seeds. The final adoption size $R(\infty)$ versus information transmission probability β with (a) $T_A = 1$; $T_B = 1$; $\rho_0 = 0.005$, (b) $T_A = 1$; $T_B = 2$; $\rho_0 = 0.03$, (c) $T_A = 1$; $T_B = 2$; $\rho_0 = 0.1$, and (d) $T_A = 1$; $T_B = 3$; $\rho_0 = 0.1$. The lines denoting theoretical solutions agree exceptionally well with the symbols representing numerical simulations. Moreover, in subgraphs (e), (f), (g), and (h), the relative variance χ in terms of the peaks numerically indicates the critical spreading probabilities in (a), (b), (c), and (d), respectively, showing that increasing the weight distribution exponent (decreasing weight distribution heterogeneity) can decrease the critical spreading probability. The phenomena above suggest that decreasing weight distribution heterogeneity facilitates information spreading but cannot alter the growth pattern of the final adoption size versus information transmission probability. The basic parameters are $N = 10^4$, $\langle k \rangle = 10$, $\langle \omega \rangle = 8$, and $\gamma = 1.0$.

not alter the growth pattern of $R(\infty)$ versus β in any pair of adoption thresholds but can promote the outbreak of information spreading. Noticeably, the theoretical solutions (lines) coincide well with the numerical simulations (symbols).

As shown in Figure 3, the initial seed size affects the information spreading dynamics. We investigate the effect of seed size on information spreading on a weighted multiplex social network, as shown in Figure 4. In Figure 4(a) ($T_A = 1; T_B = 1; \alpha_w^A = 3, \alpha_w^B = 2.5$), increasing the seed size from $\rho_0 = 0.005$ to $\rho_0 = 0.01$ not only changes the growth pattern from discontinuous to continuous, but also decreases the critical probability to promote the outbreak of information spreading. Subsequently, if the weight distribution exponent is enlarged, such as $\alpha_w^A = 3, \alpha_w^B = 3$ in Figure 4(d) and $\alpha_w^A = 3, \alpha_w^B = 3.5$ in Figure 4(g), increasing the seed size ρ_0 still advances information propagation. Comparing Figure 4(a), 4(d), and 4(g) vertically, altering the initial fraction can change the growth pattern of $R(\infty)$ versus β but cannot change the fact that increasing the weight distribution exponent (reducing weight distribution heterogeneity) retains the growth pattern while facilitating the outbreak of information spreading. Moreover, in a horizontal comparison, although enlarging the adoption thresholds, such as $T_A = 1, T_B = 2$ in Figures 4(b), 4(e), and 4(h), or $T_A = 1, T_B = 3$ in Figure 4(c), 4(f), and 4(i) renders information adoption more difficult, it is clear that increasing ρ_0 still transforms the growth pattern of $R(\infty)$ from discontinuous to continuous phase transition and promotes the outbreak of information spreading, as in the case of $T_A = 1, T_B = 1$. Additionally, changes in adoption thresholds and seed size do not qualitatively alter phenomena.

For a more comprehensive study, we obtained the results of the final adoption size on the (β, ρ_0) parameter plane, as illustrated in Figure 5. Here, we set the subgraphs in column 1 with $T_A = 1, T_B = 1$; in column 2 with $T_A = 1, T_B = 2$; in column 3 with $T_A = 1, T_B = 3$; in row 1 with $\alpha_w^A = 3, \alpha_w^B = 2.5$; in row 2 with $\alpha_w^A = 3, \alpha_w^B = 3$; and in row 3 with $\alpha_w^A = 3, \alpha_w^B = 3.5$. In the following, we discuss the findings based on Figure 5 in detail. In Figure 5(a) ($T_A = 1; T_B = 1; \alpha_w^A = 3, \alpha_w^B = 2.5$), a critical $\rho_0^* = 0.003$ exists, below which at any information transmission unit probability β no outbreak of information spreading will occur and above which outbreak and global adoption will occur. In a vertical comparison, we retain the adoption thresholds in Figures 5(a), 5(d), and 5(h) and further increase the weight distribution exponents in Figure 5(d) ($\alpha_w^A = 3, \alpha_w^B = 3$) and Figure 5(h) ($\alpha_w^A = 3, \alpha_w^B = 3.5$). The results indicate that the three subgraphs have the same critical seed size $\rho_0^* = 0.003$, below which increasing the weight distribution exponent (reducing the weight distribution heterogeneity) still cannot induce the outbreak of information spreading, but above which increasing the weight distribution exponent can accelerate the outbreak at a smaller information transmission unit probability β. Moreover, in a horizontal comparison, we retain the weight distribution exponent in Figures 5(a), 5(b), and 5(c) with $\alpha_w^A = 3, \alpha_w^B = 2.5$ and increase the adoption thresholds in Figure 5(b) ($T_A = 1, T_B = 2$) and Figure 5(c) ($T_A = 1, T_B = 3$). Under these circumstances, we discovered that the critical seed size ρ_0^* is enlarged from 0.003 to 0.06, which implies increasing the difficulty in information adoption. Analogously, other subgraphs exhibit similar findings. The phenomena in Figure 5 suggest that a critical seed size exists, above which outbreak of information spreading and global adoption will occur, and the weight distribution exponent (reducing the weight distribution heterogeneity) is essential for facilitating information spreading.

5.2. ER-SF Weighted Multiplex Networks. For cases of heterogeneous degree distributions, we investigate information spreading on a two-layered weighted ER-SF network with Poisson degree distribution $p_A(k_A) = e^{-\langle k_A \rangle} (\langle k_A \rangle^{k_A} / k_A!)$ in layer A and with power-law degree distribution $p_B(k_B) = \zeta_B k_B^{-\nu^B}$ in layer B, where $\zeta_B = 1/\sum_{k_B} k_B^{-\nu^B}$ and parameter ν^B denotes the degree exponent of layer B. Additionally, we set the minimum degree $k_B^{\min} = 4$ and maximum degree $k_B^{\max} = \sqrt{N}$.

On the weighted ER-SF networks of distinct degree distribution exponents, the growth pattern is shown in Figure 6, with the common setting $T_A = 1, T_B = 3$ in all subgraphs. In Figure 6(a) with degree distribution exponent $\nu_B = 2.1$, we discovered that enlarging the weight distribution exponent, such as from $\alpha_w^A = 3, \alpha_w^B = 2.5$ to $\alpha_w^A = 3, \alpha_w^B = 3.5$, can increase the final adoption size at the same β and decrease the critical probability to promote the outbreak of information spreading. Moreover, we proceed to increase the degree distribution exponent (reduce the degree distribution heterogeneity) in Figure 6(b) ($\nu_B = 3$) and Figure 6(c) ($\nu_B = 4$). Consequently, from Figure 6(a) to 6(c), given α_w^A and α_w^B, the growth pattern changes from continuous to the discontinuous growth pattern. However, at any given ν_B, changing the weight distribution exponent will not alter the growth pattern of $R(\infty)$. The phenomena in Figure 6 suggest that changing the degree distribution heterogeneity will not qualitatively alter the fact that reducing weight distribution heterogeneity can promote information spreading.

6. Conclusions

With the development of the Internet and mobile devices, social networks have prevailed in people's lives. Typically, an individual does not only use one social network, but multiple social networks simultaneously. Moreover, the information does not only diffuse in one social network but also spreads simultaneously on several social networks, e.g., information spreads on Twitter and Facebook simultaneously. Because of different extents of intimacy among friends, colleagues, and family members, connections in social networks should be modeled with different weights. As such, a multiplex social network should be a multilayer weighted network. Therefore, information spreading on a multiplex social network should be investigated on a multilayer weighted network. Unfortunately, the mechanism of information spreading on

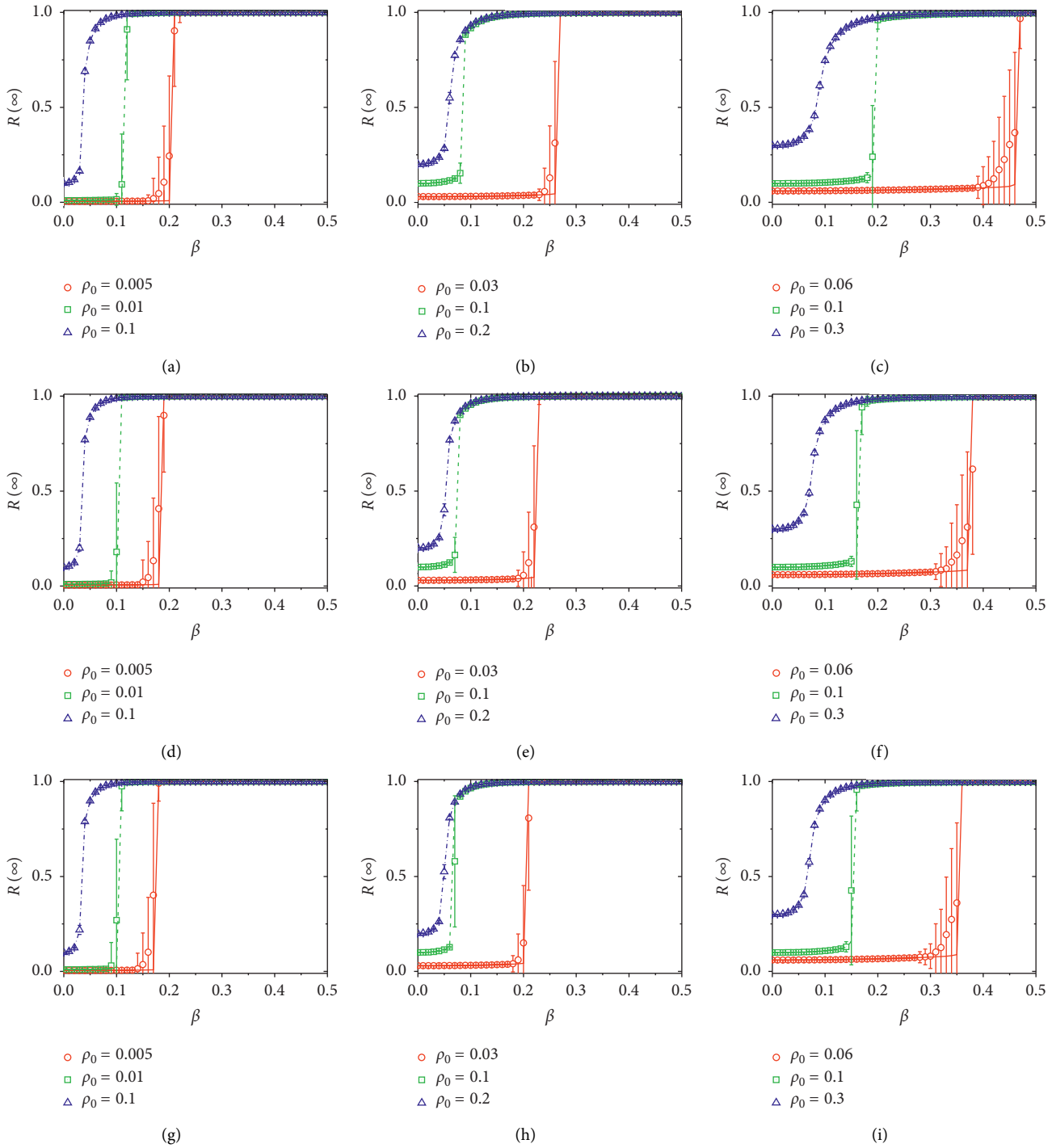

FIGURE 4: Effect of fraction of initial seeds on the growth pattern of the final adoption size $R(\infty)$ versus β on the ER-ER weighted multiplex network, under different weight distribution exponents α_ω^A and α_ω^B. The values of weight distribution exponent α_ω^A of all subgraphs are 3, and the subgraphs in each row have the same α_ω^B, i.e., subgraphs (a), (b), and (c) correspond to $\alpha_\omega^B = 2.5$; (d), (e), and (f) correspond to $\alpha_\omega^B = 3$; and (g), (h), and (i) correspond to $\alpha_\omega^B = 3.5$. Additionally, the subgraphs in each column have the same adoption threshold, i.e., subgraphs (a), (d), and (g) are set with $T_A = 1, T_B = 1$; (b), (e), and (h) with $T_A = 1, T_B = 2$; and (c), (f), and (i) with $T_A = 1, T_B = 3$. The theoretical solutions (lines) coincide well with the numerical results (symbols). Given other parameters, increasing the fraction of initial seeds will change the growth pattern of $R(\infty)$ from discontinuous to continuous growth. Moreover, vertically, increasing the weight distribution exponents (decreasing weight distribution heterogeneity) can decrease the critical transmission probability; horizontally, increasing the adoption threshold (increasing the difficulty of adoption) can contrarily enlarge the critical transmission probability. The phenomena above convey that changing the seed size can alter the growth pattern, and decreasing the adoption threshold can facilitate information spreading. Most importantly, changing the seed size of the adoption threshold cannot qualitatively alter the fact that decreasing the weight distribution heterogeneity can facilitate information spreading. The basic parameters are $N = 10^4$, $\langle k \rangle = 10$, $\langle \omega \rangle = 8$, and $\gamma = 1.0$.

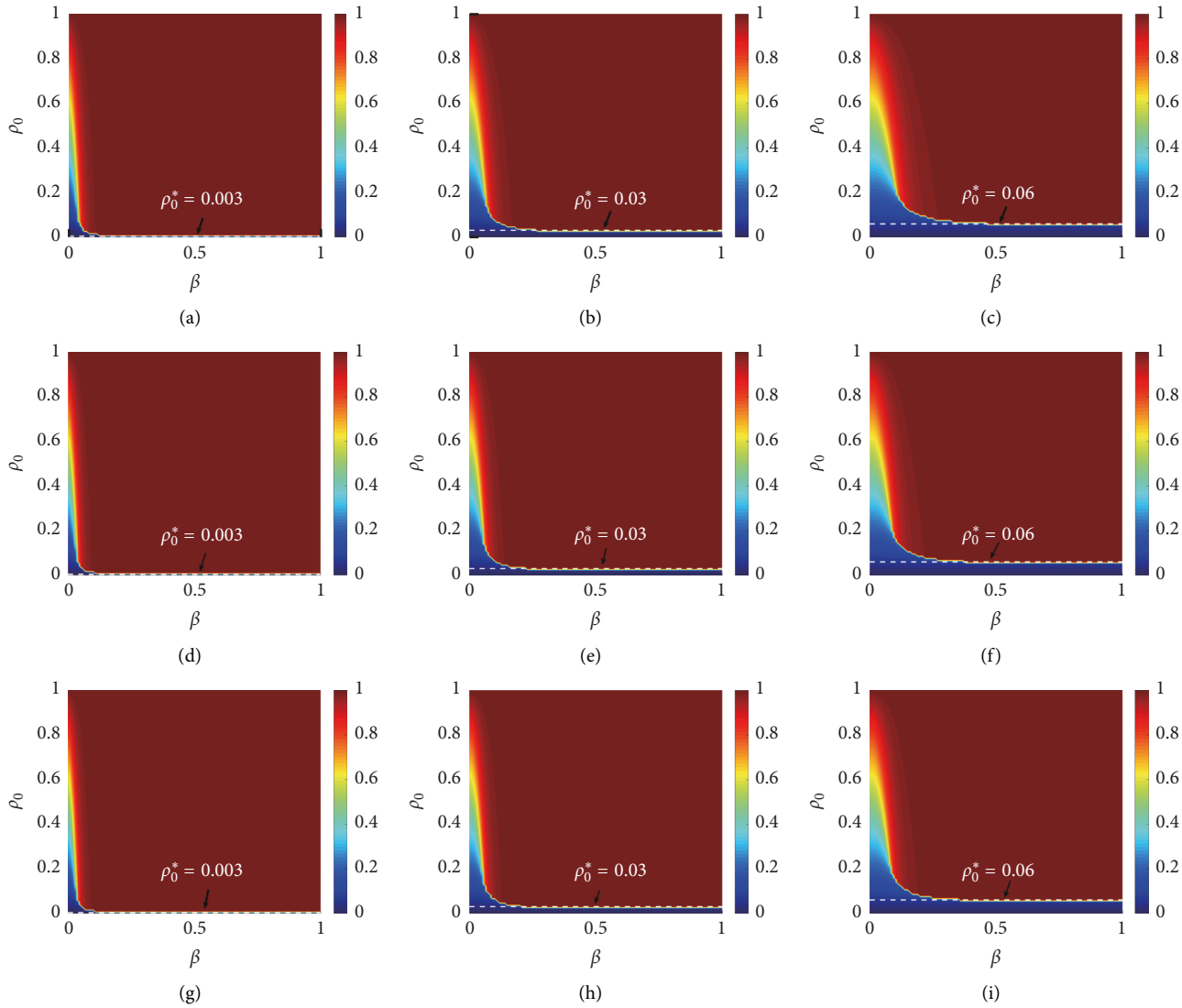

FIGURE 5: Illustrations of the growth pattern of $R(\infty)$ on the (β, ρ_0) parameter plane on the ER-ER weighted multiplex network. According to the theoretical method, the final adoption size $R(\infty)$ versus the parameter pair (β, ρ_0) was obtained. The results are plotted in subgraphs (a), (b), and (c) from row 1 with $T_A = 1, T_B = 1$; (d), (e), and (f) from row 2 with $T_A = 1, T_B = 2$; and (g), (h), and (i) from row 3 with $T_A = 1, T_B = 3$. The subgraphs have weight distribution exponents of $\alpha_\omega^A = 3$, $\alpha_\omega^B = 2.5$ in column 1; $\alpha_\omega^A = 3$, $\alpha_\omega^B = 3$ in column 2; and $\alpha_\omega^A = 3$, $\alpha_\omega^B = 3.5$ in column 3. All subgraphs show that a critical seed size ρ_0^* exists, under which no global adoption of information exists and over which a global adoption becomes possible. Additionally, the changes in the subgraphs from the first column to the third confirm that increase the weight distribution exponents (decreasing weight distribution heterogeneity) can promote information spreading. The basic parameters are $N = 10^4$, $\langle k \rangle = 10$, $\langle \omega \rangle = 8$, $\rho_0 = 0.001$, and $\gamma = 1.0$.

a weighted multiplex network has not been investigated comprehensively.

Besides, social information spreading possesses the characteristics of social reinforcement derived from the memory of nonredundant information. Herein, in terms of social reinforcement and weight distribution, we first proposed a general information spreading model on a weighted multiplex network to depict the dynamics of information spreading on a two-layered weighted network. Subsequently, we conceived a generalized edge-weight-based compartmental theory to analyze the mechanism of information spreading on a weighted multiplex network with the effect of the memory of nonredundant information. Based on the numerical method, extensive simulations confirmed that the theoretical predictions coincided well with the simulation results.

Combining numerical simulations with theoretical analyses, we discovered that under any adoption threshold of two layers, reducing weight distribution heterogeneity did not alter the growth pattern of the final adoption size but could accelerate information spreading and promote the outbreak of information spreading. Furthermore, we discovered that a critical seed size existed, below which no outbreak of information spreading occurred and above which reducing weight distribution heterogeneity was meaningful to the facilitation of information spreading. Additionally, we discovered that changing degree

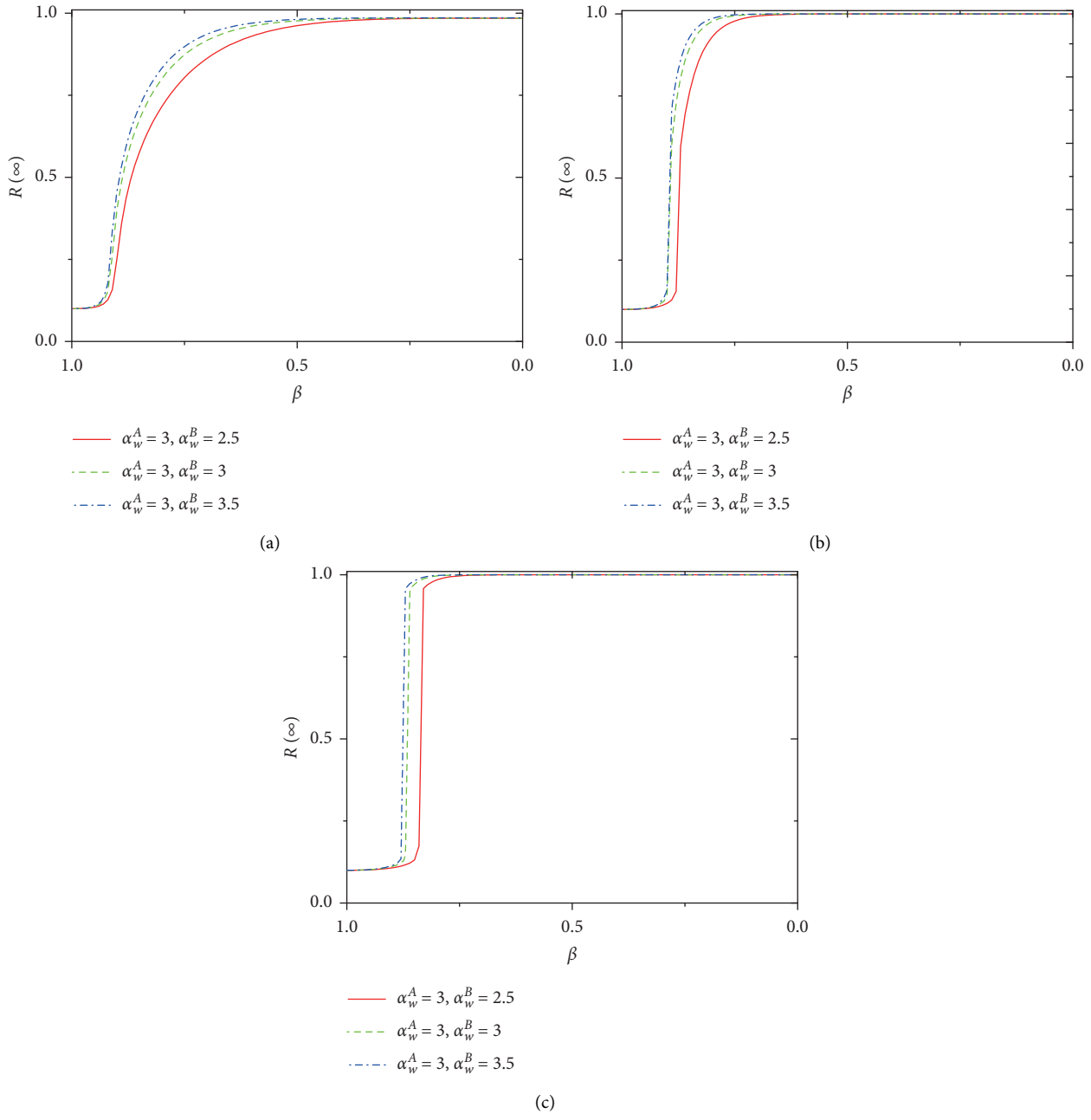

Figure 6: Effect of degree distribution heterogeneity on the final adoption size $R(\infty)$ versus β on the ER-SF weighted multiplex network with different degree distribution exponents ν_B. Subgraphs (a) ($\nu_B = 2.1$), (b) ($\nu_B = 3$), and (c) ($\nu_B = 4$) illustrate the growth patterns of $R(\infty)$ versus β under different weight distribution exponents ($\alpha_\omega^A = 3, \alpha_\omega^B = 2.5$), ($\alpha_\omega^B = 3, \alpha_\omega^B = 3$), and ($\alpha_\omega^A = 3, \alpha_\omega^B = 3.5$), respectively. From subgraphs (a)–(c), increasing the degree distribution exponent does not alter the fact that reducing the weight distribution heterogeneity (increasing the weight distribution exponent) can facilitate the spread of social behavior.

distribution heterogeneity could transform the growth pattern but did not qualitatively affect the promotion of reducing weight distribution heterogeneity to information spreading. Above all, increasing the weight distribution exponent can decrease critical transmission probability, without the influence of the degree distribution exponent.

In this study, we unveiled the effect of weighted multiplex network structures on information spreading. This study can inspire further studies related to the design of optimized strategies to control information spreading on multiplex social networks. Additionally, more accurate theories to depict the social contagion on real two-layer coupled networks should be further explored.

Data Availability

The data used to support the findings of this study are available from the corresponding author upon request.

Conflicts of Interest

The authors declare that they have no conflicts of interest.

Acknowledgments

This work was supported by the National Natural Science Foundation of China (nos. 61602048, and 61673086) and the Fundamental Research Funds of the Central Universities.

References

[1] G.-Q. Zhang, G.-Q. Zhang, Q.-F. Yang, S.-Q. Cheng, and T. Zhou, "Evolution of the Internet and its cores," *New Journal of Physics*, vol. 10, no. 12, Article ID 123027, 2008.

[2] S. Anand, M. Venkataraman, K. P. Subbalakshmi, and R. Chandramouli, "Spatio-temporal analysis of passive consumption in internet media," *IEEE Transactions on Knowledge and Data Engineering*, vol. 27, no. 10, pp. 2839–2850, 2015.

[3] T. O'Reilly, "What is web 2.0: design patterns and business models for the next generation of software," 2007, http://www.oreilly.com/pub/a/web2/archive/what-is-web-20.html.

[4] G. Goggin, *Cell Phone Culture: Mobile Technology in Everyday Life*, Routledge, Abingdon, UK, 2006.

[5] Y. Dong, N. V. Chawla, J. Tang, and Y. Yang, "User modeling on demographic attributes in big mobile social networks," *ACM Transactions on Information Systems*, vol. 35, no. 4, pp. 1–33, 2017.

[6] A. Macarthy, *500 Social Media Marketing Tips: Essential Advice, Hints and Strategy for Business Facebook, Twitter, Pinterest, Google+, YouTube, Instagram, LinkedIn, and More!*, CreateSpace Independent Publishing Platform, Scotts Valley, CA, USA, 2018.

[7] S. F. Waterloo, S. E. Baumgartner, J. Peter, and P. M. Valkenburg, "Norms of online expressions of emotion: comparing facebook, twitter, instagram, and whatsapp," *New Media & Society*, vol. 20, no. 5, pp. 1813–1831, 2018.

[8] J. Cao, Z. Bu, Y. Wang, H. Yang, J. Jiang, and H.-J. Li, "Detecting prosumer-community groups in smart grids from the multiagent perspective," *IEEE Transactions on Systems, Man, and Cybernetics: Systems*, vol. 49, no. 8, pp. 1652–1664, 2019.

[9] M. D. Vicario, F. Zollo, G. Caldarelli, A. Scala, and W. Quattrociocchi, "Mapping social dynamics on facebook: the brexit debate," *Social Networks*, vol. 50, pp. 6–16, 2017.

[10] B. J. Jansen, M. Zhang, K. Sobel, and A. Chowdury, "Twitter power: tweets as electronic word of mouth," *Journal of the American Society for Information Science and Technology*, vol. 60, no. 11, pp. 2169–2188, 2009.

[11] D. Yu, N. Chen, and X. Ran, "Computational modeling of Weibo user influence based on information interactive network," *Online Information Review*, vol. 40, no. 7, pp. 867–881, 2016.

[12] C. Ju and W. Tao, "Relationship strength estimation based on Wechat Friends Circle," *Neurocomputing*, vol. 253, pp. 15–23, 2017.

[13] D. Li, S. Zhang, X. Sun, H. Zhou, S. Li, and X. Li, "Modeling information diffusion over social networks for temporal dynamic prediction," *IEEE Transactions on Knowledge and Data Engineering*, vol. 29, no. 9, pp. 1985–1997, 2017.

[14] L. Wu, Y. Ge, Q. Liu et al., "Modeling the evolution of users' preferences and social links in social networking services," *IEEE Transactions on Knowledge and Data Engineering*, vol. 29, no. 6, pp. 1240–1253, 2017.

[15] S. Vosoughi, D. Roy, and S. Aral, "The spread of true and false news online," *Science*, vol. 359, no. 6380, pp. 1146–1151, 2018.

[16] X. Zhu, H. Tian, X. Chen, W. Wang, and S. Cai, "Heterogeneous behavioral adoption in multiplex networks," *New Journal of Physics*, vol. 20, no. 12, Article ID 125002, 2018.

[17] S. V. Jin, ""Celebrity 2.0 and beyond!" Effects of Facebook profile sources on social networking advertising," *Computers in Human Behavior*, vol. 79, pp. 154–168, 2018.

[18] A. Song, Y. Liu, Z. Wu, M. Zhai, and J. Luo, "A local random walk model for complex networks based on discriminative feature combinations," *Expert Systems with Applications*, vol. 118, pp. 329–339, 2019.

[19] D. Centola, "An experimental study of homophily in the adoption of health behavior," *Science*, vol. 334, no. 6060, pp. 1269–1272, 2011.

[20] Z. Bu, Y. Wang, H.-J. Li, J. Jiang, Z. Wu, and J. Cao, "Link prediction in temporal networks: integrating survival analysis and game theory," *Information Sciences*, vol. 498, pp. 41–61, 2019.

[21] H. P. Young, "The dynamics of social innovation," *Proceedings of the National Academy of Sciences*, vol. 108, no. 4, pp. 21285–21291, 2011.

[22] M. E. J. Newman, S. Forrest, and J. Balthrop, "Email networks and the spread of computer viruses," *Physical Review E*, vol. 66, no. 3, Article ID 035101, 2002.

[23] Z. Wang, C. T. Bauch, S. Bhattacharyya et al., "Statistical physics of vaccination," *Physics Reports*, vol. 664, pp. 1–113, 2016.

[24] Z. Wang, Y. Moreno, S. Boccaletti, and M. Perc, "Vaccination and epidemics in networked populations–an introduction," *Chaos, Solitons & Fractals*, vol. 103, pp. 177–183, 2017.

[25] Y. Zhang, S. Zhou, Z. Zhang, J. Guan, and S. Zhou, "Rumor evolution in social networks," *Physical Review E*, vol. 87, no. 3, 2013.

[26] A. Banerjee, A. G. Chandrasekhar, E. Duflo, and M. O. Jackson, "The diffusion of microfinance," *Science*, vol. 341, no. 6144, Article ID 1236498, 2013.

[27] S. Jiang, H. Fan, and M. Xia, "Credit risk contagion based on asymmetric information association," *Complexity*, vol. 2018, Article ID 2929157, 11 pages, 2018.

[28] D. J. Watts and P. S. Dodds, "Influentials, networks, and public opinion formation," *Journal of Consumer Research*, vol. 34, no. 4, pp. 441–458, 2007.

[29] X. Liu, C. Liu, and X. Zeng, "Online social network emergency public event information propagation and nonlinear mathematical modeling," *Complexity*, vol. 2017, Article ID 5857372, 7 pages, 2017.

[30] M. Gutiérrez-Roig, O. Sagarra, A. Oltra et al., "Active and reactive behaviour in human mobility: the influence of attraction points on pedestrians," *Royal Society Open Science*, vol. 3, no. 7, Article ID 160177, 2016.

[31] C. Liu, X.-X. Zhan, Z.-K. Zhang, G.-Q. Sun, and P. M. Hui, "How events determine spreading patterns: information transmission via internal and external influences on social networks," *New Journal of Physics*, vol. 17, no. 11, Article ID 113045, 2015.

[32] Z.-K. Zhang, C. Liu, X.-X. Zhan, X. Lu, C.-X. Zhang, and Y.-C. Zhang, "Dynamics of information diffusion and its applications on complex networks," *Physics Reports*, vol. 651, pp. 1–34, 2016.

[33] M. E. J. Newman, "The structure and function of complex networks," *SIAM Review*, vol. 45, no. 2, pp. 167–256, 2003.

[34] M. Newman, *Networks*, Oxford University Press, Oxford, UK, 2018.

[35] C. Castellano, S. Fortunato, and V. Loreto, "Statistical physics of social dynamics," *Reviews of Modern Physics*, vol. 81, no. 2, pp. 591–646, 2009.

[36] J. P. Gleeson and D. J. Cahalane, "Seed size strongly affects cascades on random networks," *Physical Review E*, vol. 75, no. 5, Article ID 056103, 2007.

[37] D. E. Whitney, "Dynamic theory of cascades on finite clustered random networks with a threshold rule," *Physical Review E*, vol. 82, no. 6, Article ID 066110, 2010.

[38] A. Nematzadeh, E. Ferrara, A. Flammini, and Y. Ahn, "Optimal network modularity for information diffusion," *Physical Review Letters*, vol. 113, no. 25, Article ID 088701, 2014.

[39] M. Liu, W. Wang, Y. Liu, M. Tang, S. Cai, and H. Zhang, "Social contagions on time-varying community networks," *Physical Review E*, vol. 95, no. 5, 2017.

[40] Q. H. Liu, W. Wang, M. Tang, T. Zhou, and Y. Lai, "Explosive spreading on complex networks: the role of synergy," *Physical Review E*, vol. 95, no. 4, Article ID 042320, 2017.

[41] W. Wang, Q. Liu, J. Liang, Y. Hu, and T. Zhou, "Coevolution Spreading in Complex Networks," *Physics and Society*, vol. 820, pp. 1–51, 2019.

[42] W. Wang, M. Tang, P. Shu, and Z. Wang, "Dynamics of social contagions with heterogeneous adoption thresholds: crossover phenomena in phase transition," *New Journal of Physics*, vol. 18, no. 1, Article ID 013029, 2016.

[43] P. S. Dodds, K. D. Harris, and C. M. Danforth, "Limited imitation contagion on random networks: chaos, universality, and unpredictability," *Physical Review Letters*, vol. 110, no. 15, Article ID 158701, 2013.

[44] X. Zhu, W. Wang, S. Cai, and H. E. Stanley, "Optimal imitation capacity and crossover phenomenon in the dynamics of social contagions," *Journal of Statistical Mechanics: Theory and Experiment*, vol. 2018, no. 6, Article ID 063405, 2018.

[45] X. Zhu, W. Wang, S. Cai, and H. E. Stanley, "Dynamics of social contagions with local trend imitation," *Scientific Reports*, vol. 8, no. 1, p. 7335, 2018.

[46] Z. Wang, A. Szolnoki, and M. Perc, "Optimal interdependence between networks for the evolution of cooperation," *Scientific Reports*, vol. 3, no. 1, p. 2470, 2013.

[47] Z. Wang, A. Szolnoki, and M. Perc, "Self-organization towards optimally interdependent networks by means of coevolution," *New Journal of Physics*, vol. 16, no. 3, Article ID 033041, 2014.

[48] E. Cozzo, M. Kivelä, M. De Domenico et al., "Structure of triadic relations in multiplex networks," *New Journal of Physics*, vol. 17, no. 7, Article ID 073029, 2015.

[49] W. Wang, M. Tang, H. E. Stanley, and L. A. Braunstein, "Social contagions with communication channel alternation on multiplex networks," *Physical Review E*, vol. 98, no. 6, 2018.

[50] R. Amato, N. E. Kouvaris, M. S. Miguel, and A. Díaz-Guilera, "Opinion competition dynamics on multiplex networks," *New Journal of Physics*, vol. 19, no. 12, Article ID 123019, 2017.

[51] W. Li, S. Tang, W. Fang, Q. Guo, X. Zhang, and Z. Zheng, "How multiple social networks affect user awareness: the information diffusion process in multiplex networks," *Physical Review E*, vol. 92, no. 4, Article ID 042810, 2015.

[52] X. Chen, R. Wang, M. Tang, S. Cai, H. E. Stanley, and L. A. Braunstein, "Suppressing epidemic spreading in multiplex networks with social-support," *New Journal of Physics*, vol. 20, no. 1, Article ID 013007, 2018.

[53] R. Amato, A. Diaz-Guilera, and K.-K. Kleineberg, "Interplay between social influence and competitive strategical games in multiplex networks," *Scientific Reports*, vol. 7, no. 1, p. 7087, 2017.

[54] R. J. Requejo and A. Diaz-Guilera, "Replicator dynamics with diffusion on multiplex networks," *Physical Review E*, vol. 94, no. 2, Article ID 022301, 2016.

[55] M. Zheng, L. Lü, and M. Zhao, "Spreading in online social networks: the role of social reinforcement," *Physical Review E*, vol. 88, no. 1, Article ID 012818, 2013.

[56] E. M. Tur, P. Zeppini, and K. Frenken, "Diffusion with social reinforcement: the role of individual preferences," *Physical Review E*, vol. 97, no. 2, Article ID 002300, 2018.

[57] W. Wang, M. Tang, H.-F. Zhang, and Y.-C. Lai, "Dynamics of social contagions with memory of nonredundant information," *Physical Review E*, vol. 92, no. 1, Article ID 012820, 2015.

[58] S. Boccaletti, V. Latora, Y. Moreno, M. Chavez, and D. Hwang, "Complex networks: structure and dynamics," *Physics Reports*, vol. 424, no. 4-5, pp. 175–308, 2006.

[59] Y. Sun, C. Liu, C.-X. Zhang, and Z.-K. Zhang, "Epidemic spreading on weighted complex networks," *Physics Letters A*, vol. 378, no. 7-8, pp. 635–640, 2014.

[60] A. Barrat, M. Barthelemy, R. Pastor-Satorras, and A. Vespignani, "The architecture of complex weighted networks," *Proceedings of the National Academy of Sciences*, vol. 101, no. 11, pp. 3747–3752, 2004.

[61] Y. Zhu, W. Wang, M. Tang, and Y. Ahn, "Social contagions on weighted networks," *Physical Review E*, vol. 96, no. 1, 2017.

[62] M. Catanzaro, M. Boguñá, and R. Pastor-Satorras, "Generation of uncorrelated random scale-free networks," *Physical Review E*, vol. 71, no. 2, Article ID 027103, 2004.

[63] R. Pastor-Satorras and A. Vespignani, "Epidemic spreading in scale-free networks," *Physical Review Letters*, vol. 86, no. 14, pp. 3200–3203, 2001.

[64] X.-X. Zhan, C. Liu, G. Zhou et al., "Coupling dynamics of epidemic spreading and information diffusion on complex networks," *Applied Mathematics and Computation*, vol. 332, pp. 437–448, 2018.

[65] J. C. Miller and E. M. Volz, "Model hierarchies in edge-based compartmental modeling for infectious disease spread," *Journal of Mathematical Biology*, vol. 67, no. 4, pp. 869–899, 2013.

[66] J. C. Miller and E. M. Volz, "Incorporating disease and population structure into models of sir disease in contact networks," *PLoS One*, vol. 8, no. 8, Article ID e69162, 2013.

[67] K. Brian and M. E. J. Newman, "Message passing approach for general epidemic models," *Physical Review E*, vol. 82, no. 1, Article ID 016101, 2010.

[68] X. Yuan, Y. Hu, H. E. Stanley, and S. Havlin, "Eradicating catastrophic collapse in interdependent networks via reinforced nodes," *Proceedings of the National Academy of Sciences*, vol. 114, no. 13, pp. 3311–3315, 2017.

[69] P. Erdös and A. Rényi, "On random graphs i," *Publicationes Mathematicae*, vol. 4, pp. 3286–3291, 1959.

[70] P. Shu, Q.-H. Liu, S. Wang, and W. Wang, "Social contagions on interconnected networks of heterogeneous populations," *Chaos: An Interdisciplinary Journal of Nonlinear Science*, vol. 28, no. 11, Article ID 113114, 2018.